



# Active Vision: Range Data Chapter 12.2/12.3 Szelisky CV

Guido Gerig  
CS 6320, Spring 2012

(credit: some slides from F&P book Computer  
Vision)



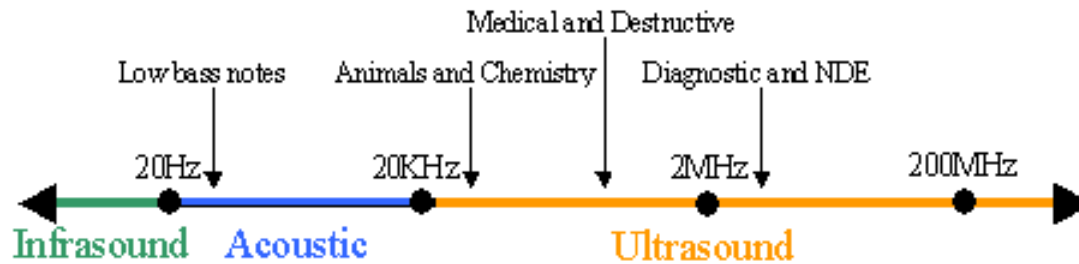
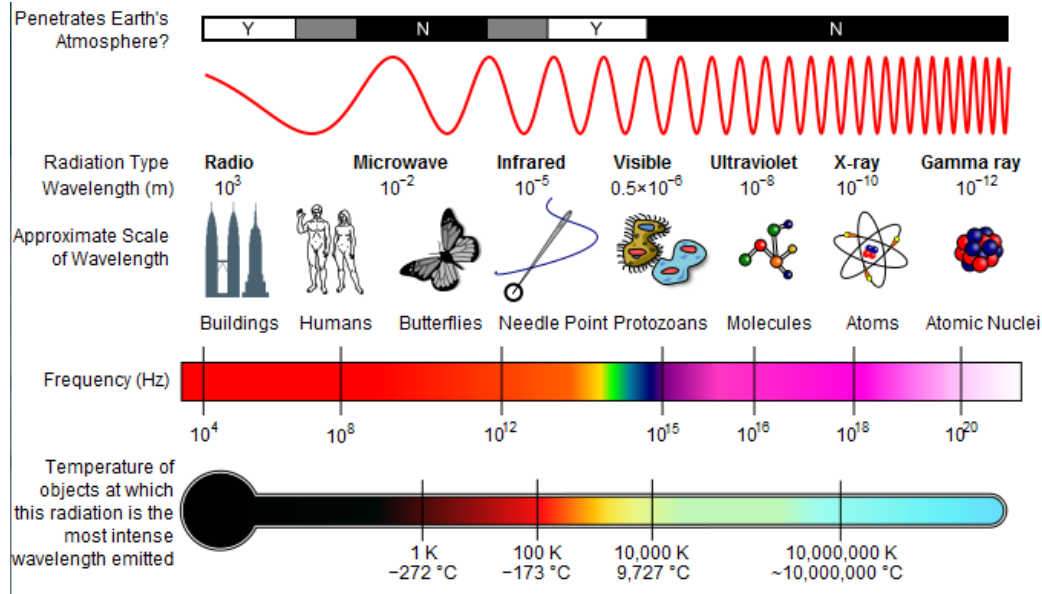
# Contents

- Range cameras and physical principle
- Processing of range image data
  - Patches of homogeneous properties
  - Extended Gaussian Image (EGI)
  - Discontinuities: Local curvatures
  - Registration of Range Data: ICP
- Applications

Material: Szelisky coursebook Computer Vision  
12.2/12/3

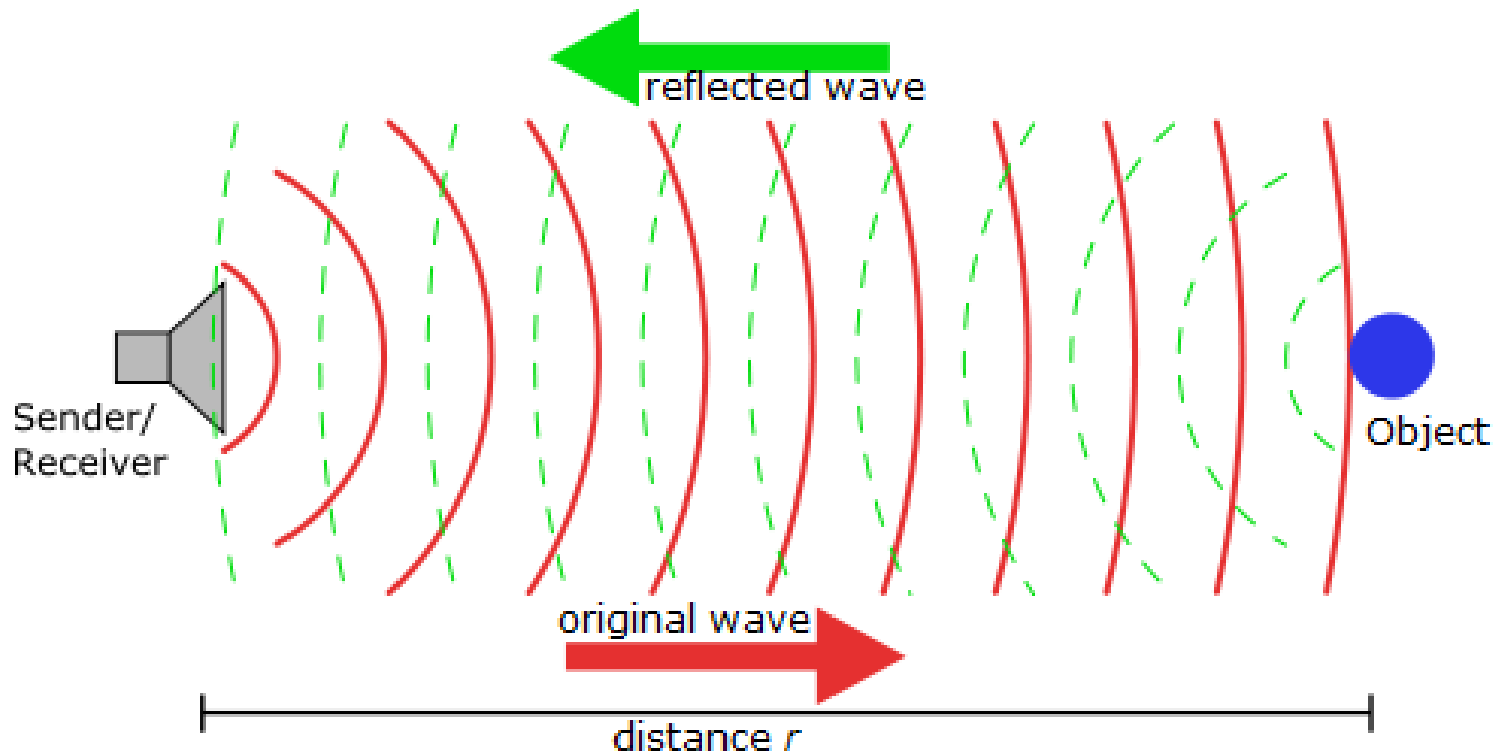


# Physical Principles



Source: Wikipedia

# SONAR (Sound navigation and ranging)



**Principle:** Wave with known velocity  $v$  traveling distance  $2*r$  → takes time  $t_f$



# Bats

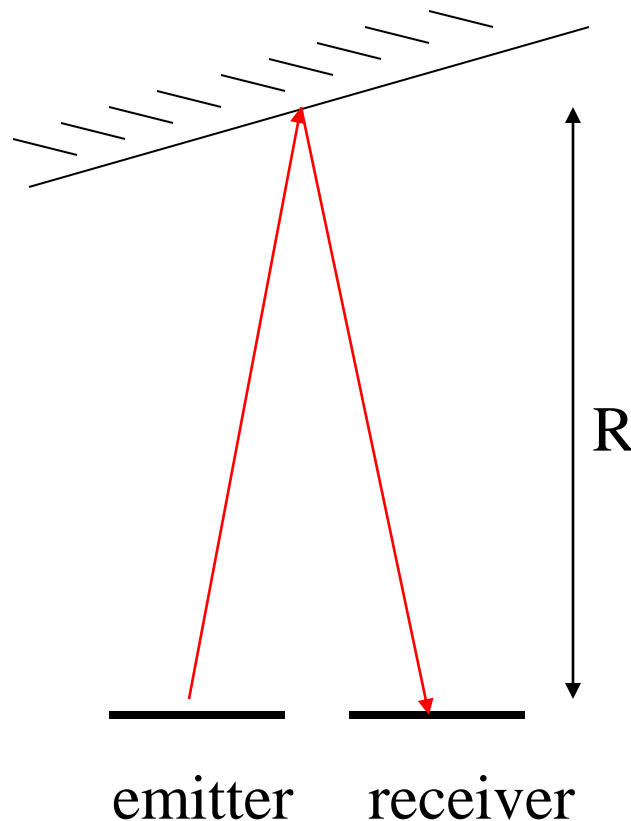


Bats use a variety of ultrasonic ranging (echolocation) techniques to detect their prey. They can detect frequencies as high as 100 kHz, although there is some disagreement on the upper limit.<sup>[22]</sup> (see also dolphins, shrews, whales).



# Time of Flight (TOF)

**Basic principle: Time of Flight (TOF): Emit signal, wait for echo, measure time difference**



Range measurement:

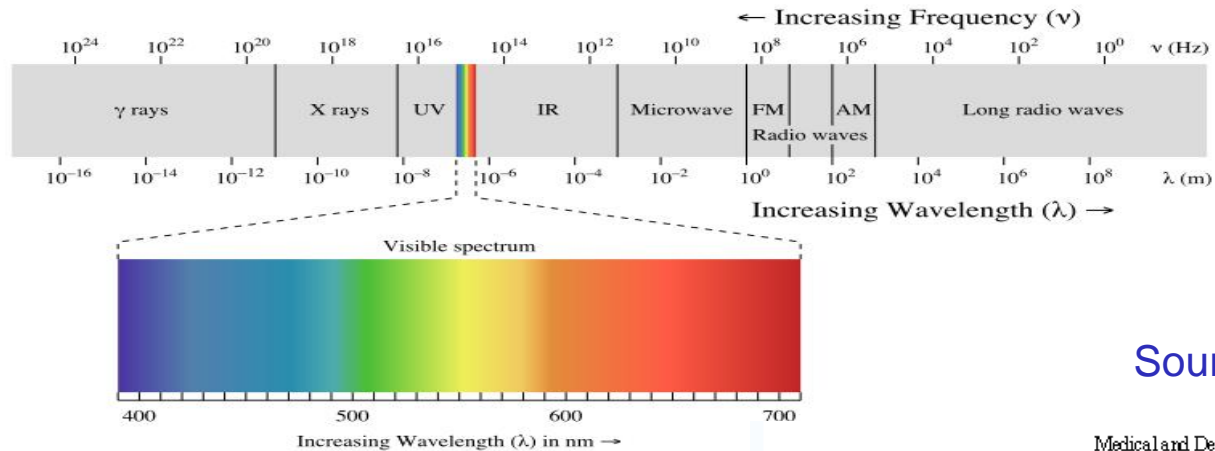
- Velocity  $v$  is known
- $t_f$  to be measured

$$2R = v * t_f$$

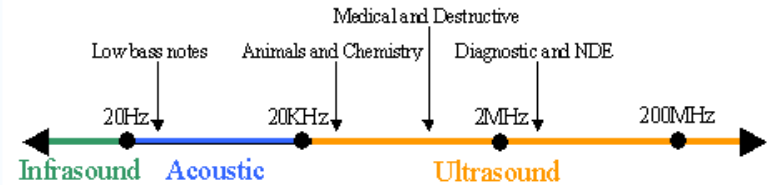
$$R = \frac{v * t_f}{2}$$



# Wavelengths for TOF



Source: Wikipedia



- Radar (microwaves:  $c=c_{\text{light}}$ ,  $\lambda = 0.02\text{m}$ ,  $f = 15\text{GHz}$ )
- Light/Laser (light:  $c_{\text{light}} = 3 \times 10^8 \text{ m/sec}$ ,  $\lambda = 400\text{nm}$  to  $700\text{nm}$ ,  $f = 7$  to  $4 \times 10^6 \text{ GHz}$ )
- Sound (sound:  $c = 331 \text{ m/sec}$ ,  $\lambda = 0.02\text{m}$ ,  $f = 20\text{Hz}$  to  $20\text{kHz}$ )
- Ultrasound (sound:  $c = 331 \text{ m/sec}$ ,  $\lambda = 0.017\text{mm}$ ,  $f = 2\text{MHz}$ )



# TOF ctd.

Resolution:  
Challenge for  
electronics:

$$t_f = \frac{2 * R}{v}$$

$$\Delta t_f = \frac{2 * \Delta R}{v}$$

Example:

- Sound:  
 $v = 330 \text{ m/sec}$   
 $\Delta R = 1 \text{ cm} \rightarrow$   
 $\Delta t = 60 \mu\text{s}$
- Light:  
 $c = 3 * 10^8 \text{ m/sec}$   
 $\Delta R = 1 \text{ cm} \rightarrow$   
 $\Delta t = 67 \text{ ps}$   
(picoseconds)



# Ultrasound



- Example: **Polaroid**
- Material or topology may absorb arbitrary frequencies: Transmits several frequencies (Polaroid: 60,57,53,50kHz)
- Engineering principle: Use pulsed frequency ( $f$ ) and digital counter ( $n$ )
- Range of counter:  $2^k-1$  (e.g. 16bit)
- Range of unique depth measurement:  $R^*$
- Example:  $f=50\text{kHz}$ ,  $v=330\text{m/sec}$ ,  $k=16$ :  $R^*=216\text{m}$ , 1count: 6.6mm)
- Problem: wide bundle ( $30^\circ$ )



$$t_f = \frac{n}{f}$$

$$R = \frac{t_f * v}{2} = \frac{n * v}{2f}$$

$$R^* = \frac{(2^k - 1) * v}{2f}$$



# Pulsed Time of Flight

- Advantages:
  - Large working volume (up to 100 m.)
- Disadvantages:
  - Not-so-great accuracy (at best  $\sim 5$  mm.)
    - Requires getting timing to  $\sim 30$  picoseconds
    - Does not scale with working volume
- Often used for scanning buildings, rooms, archeological sites, etc.



# Laser

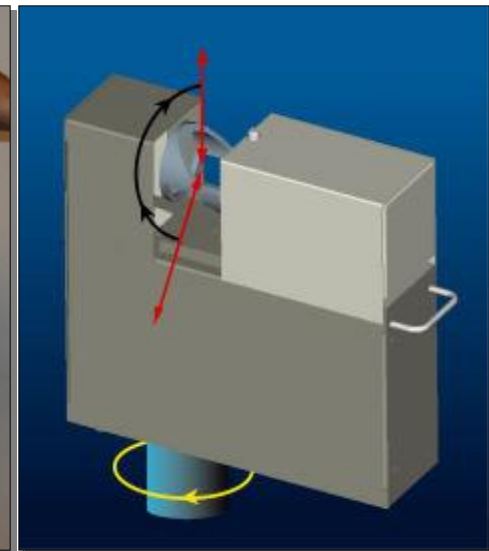
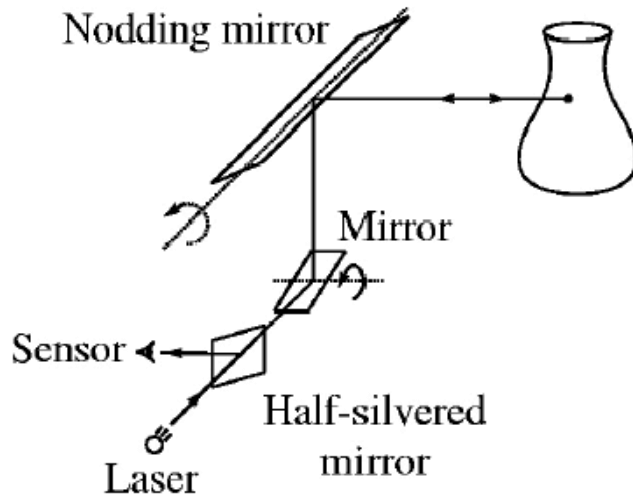
- Very narrow bundle: high spatial resolution
- But: High temporal resolution of measurement electronics (pico-seconds)
- Example: 1cm depth resolution: 70 pico sec
- Reliable measurements: Large #pulses
- Alternative to TOF:
  - Phase Shift encoding
  - Modulation of laser with sin-wave of frequency  $f_{AM}$
  - Phase shift due to time of flight



# Pulsed Time of Flight

- Basic idea: send out pulse of light (usually laser), time how long it takes to return

$$d = \frac{1}{2} c \Delta t$$





# Depth cameras

2D array of  
time-of-flight  
sensors

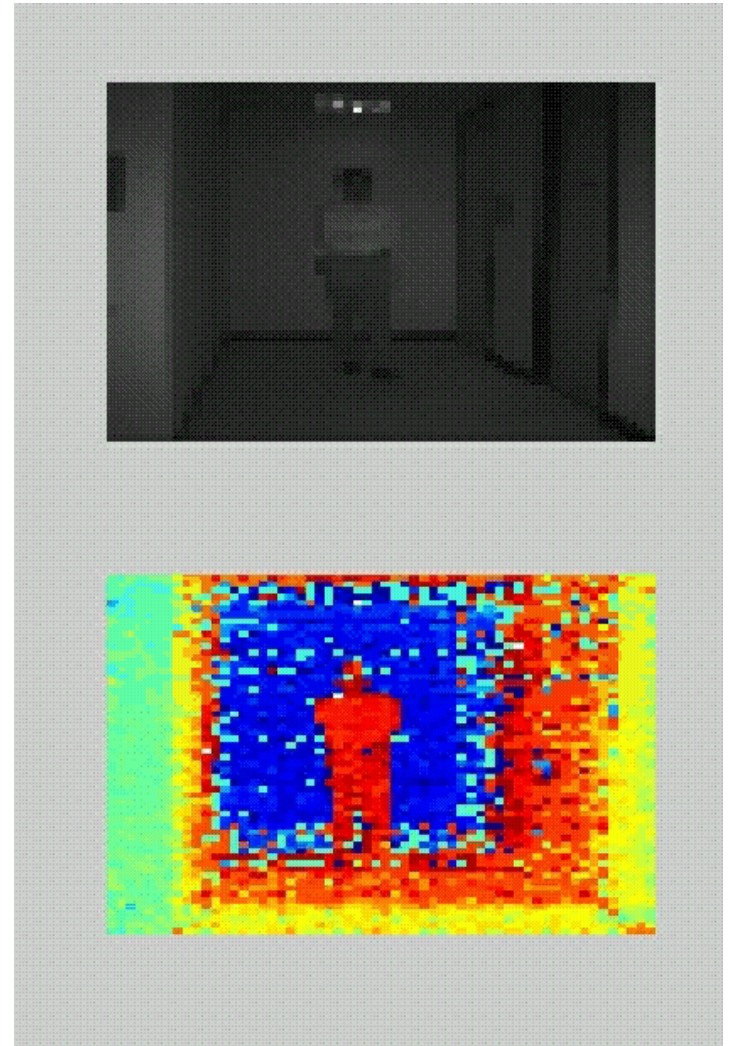
e.g. Canesta's CMOS 3D  
sensor

jitter too big on single  
measurement,  
but averages out on many  
(10,000 measurements  $\Rightarrow$  100x  
improvement)

Canesta: Principle: <http://en.wikipedia.org/wiki/Canesta>

Demo:

[http://www.youtube.com/watch?v=5\\_PVx1NbUZQ&noredirect=1](http://www.youtube.com/watch?v=5_PVx1NbUZQ&noredirect=1)



# Range Image Data

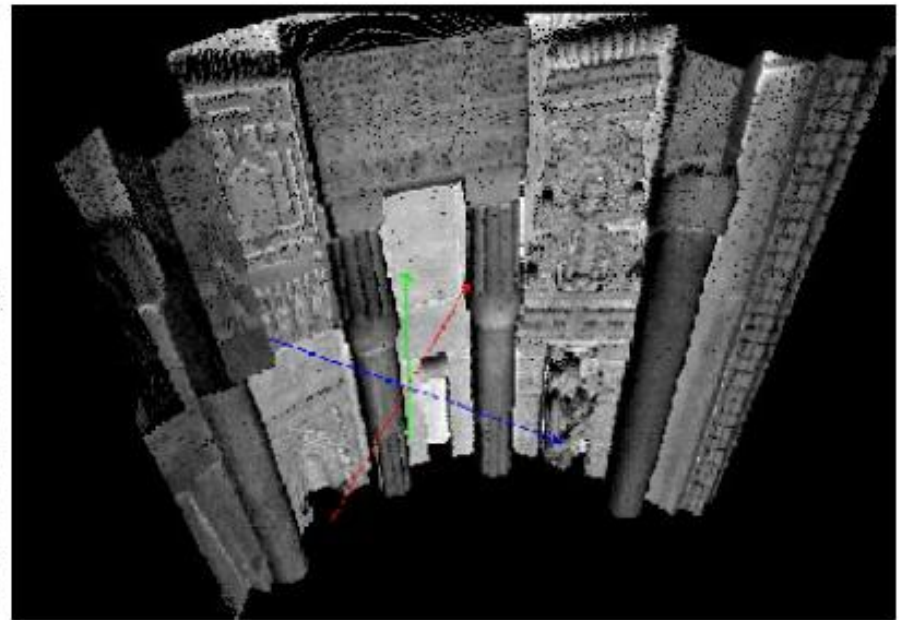
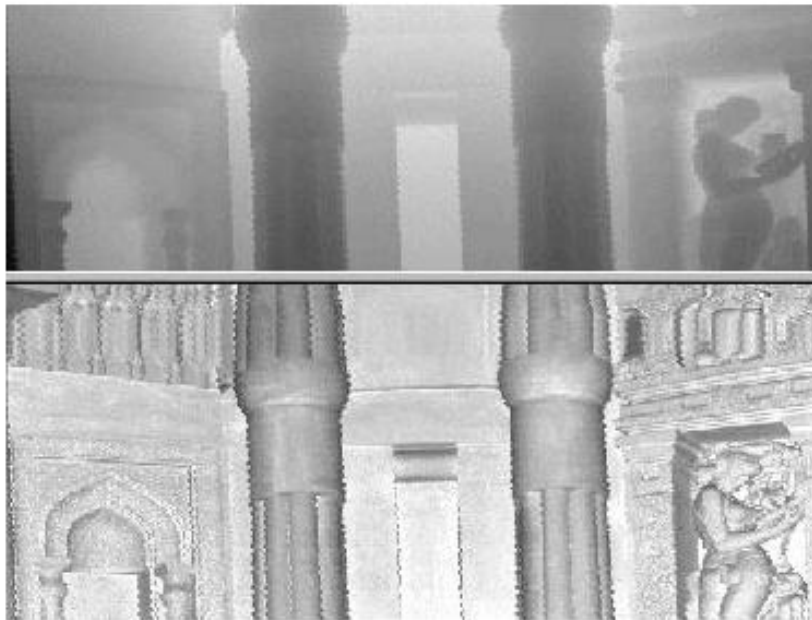


**Figure 24.3.** Range data captured by the AM phase shift range finder described in [Hancock *et al.*, 1998]: (left) range and intensity images; (right) perspective plot of the range data. Reprinted from [Hebert, 2000], Figure 5.

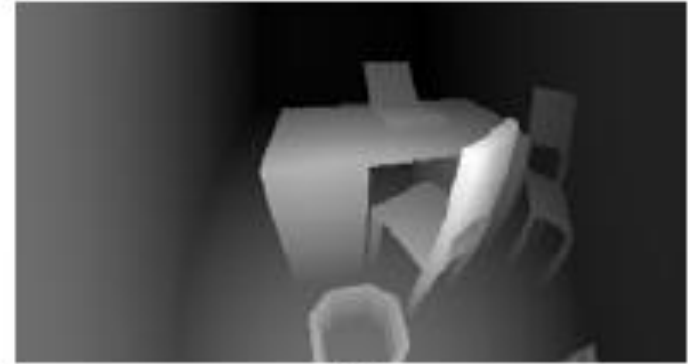




# Input Data



(a)



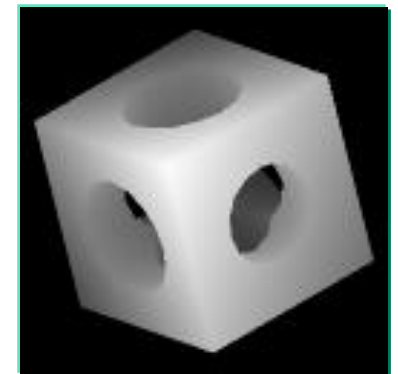
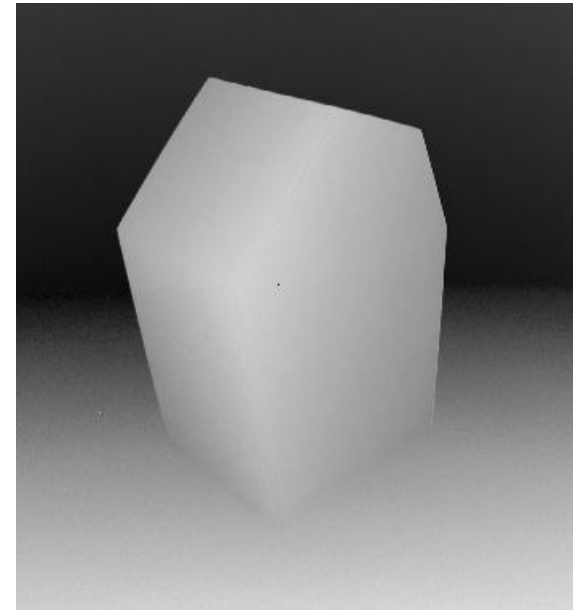
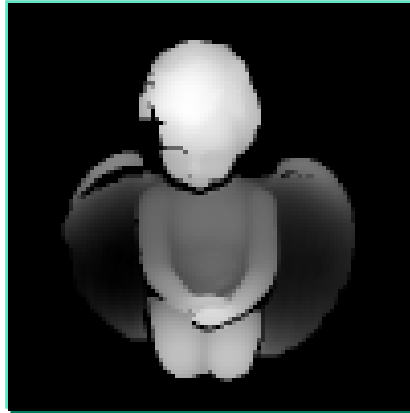
(b)



(c)

Simulated and real range images

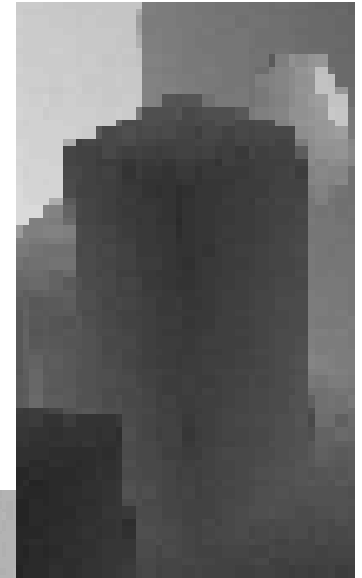
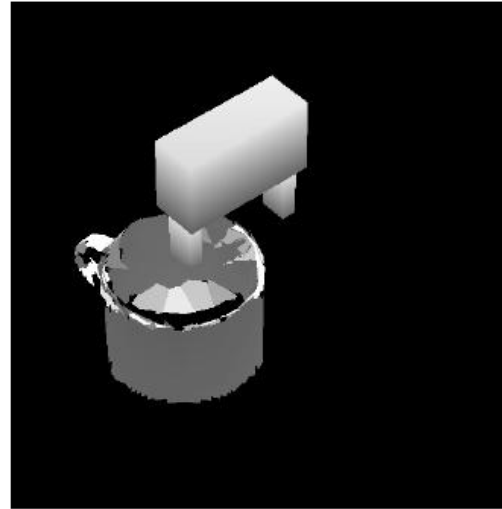
# What is special about range images?



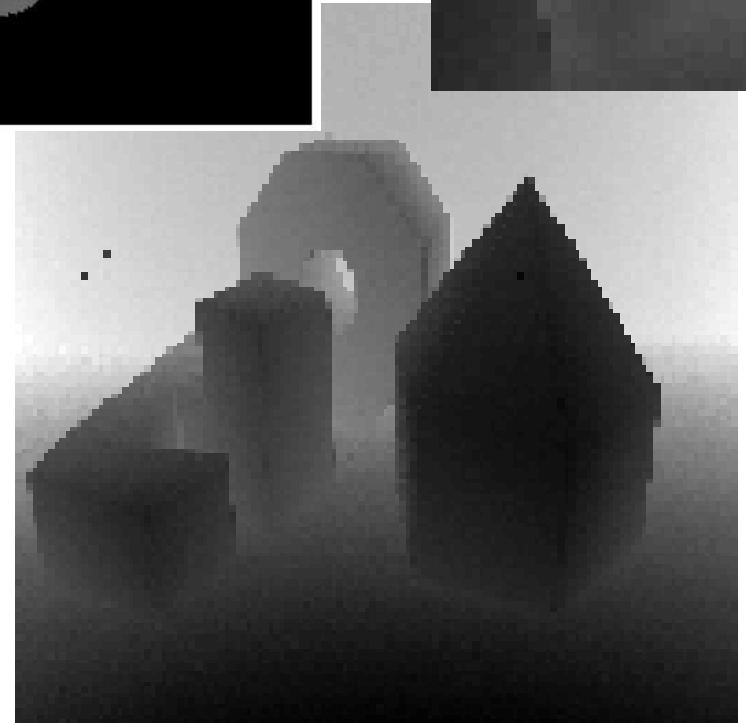
Object faces?  
Object boundaries?



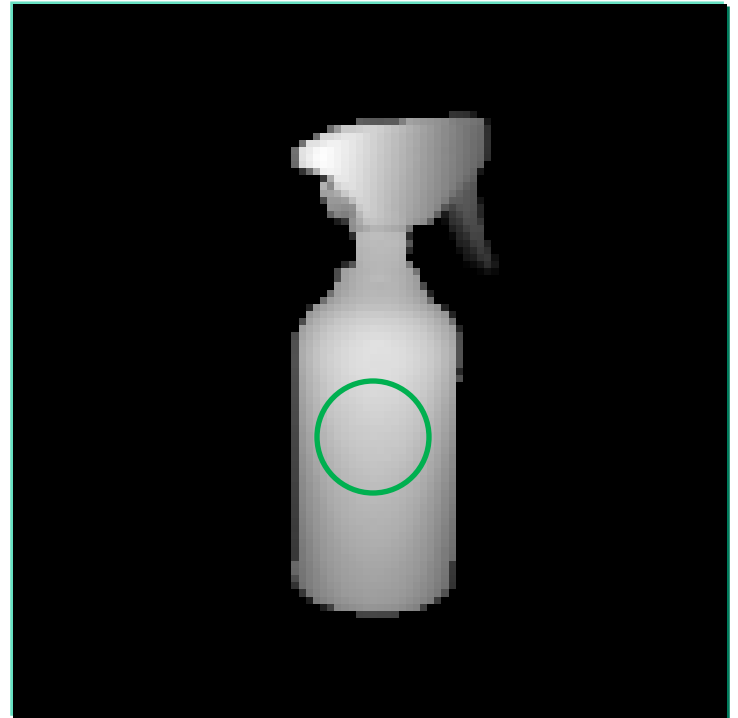
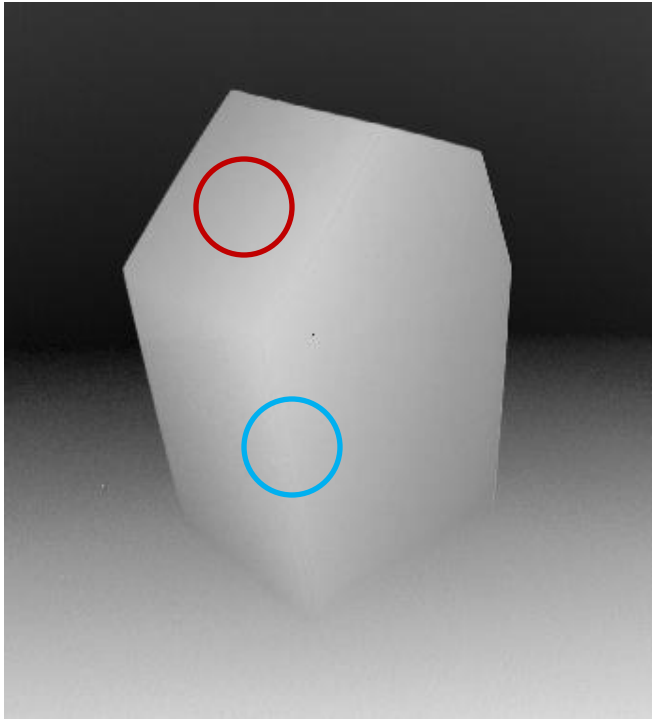
# What is different in range images?



Object faces?  
Object boundaries?

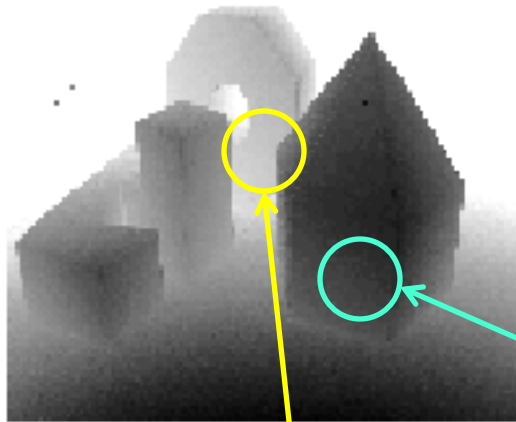


# What is special about range images?

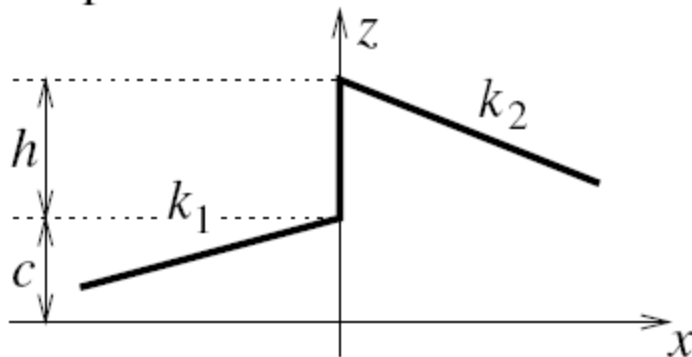


- Homogeneous in surface normals
- Crest line: Abrupt change of surface normals
- Continuous change of normals, homogeneous in curvature

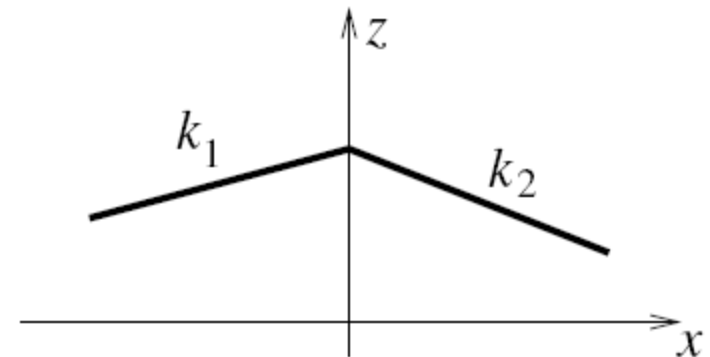
# Types of Discontinuities in Range Images



Step Model



Roof Model

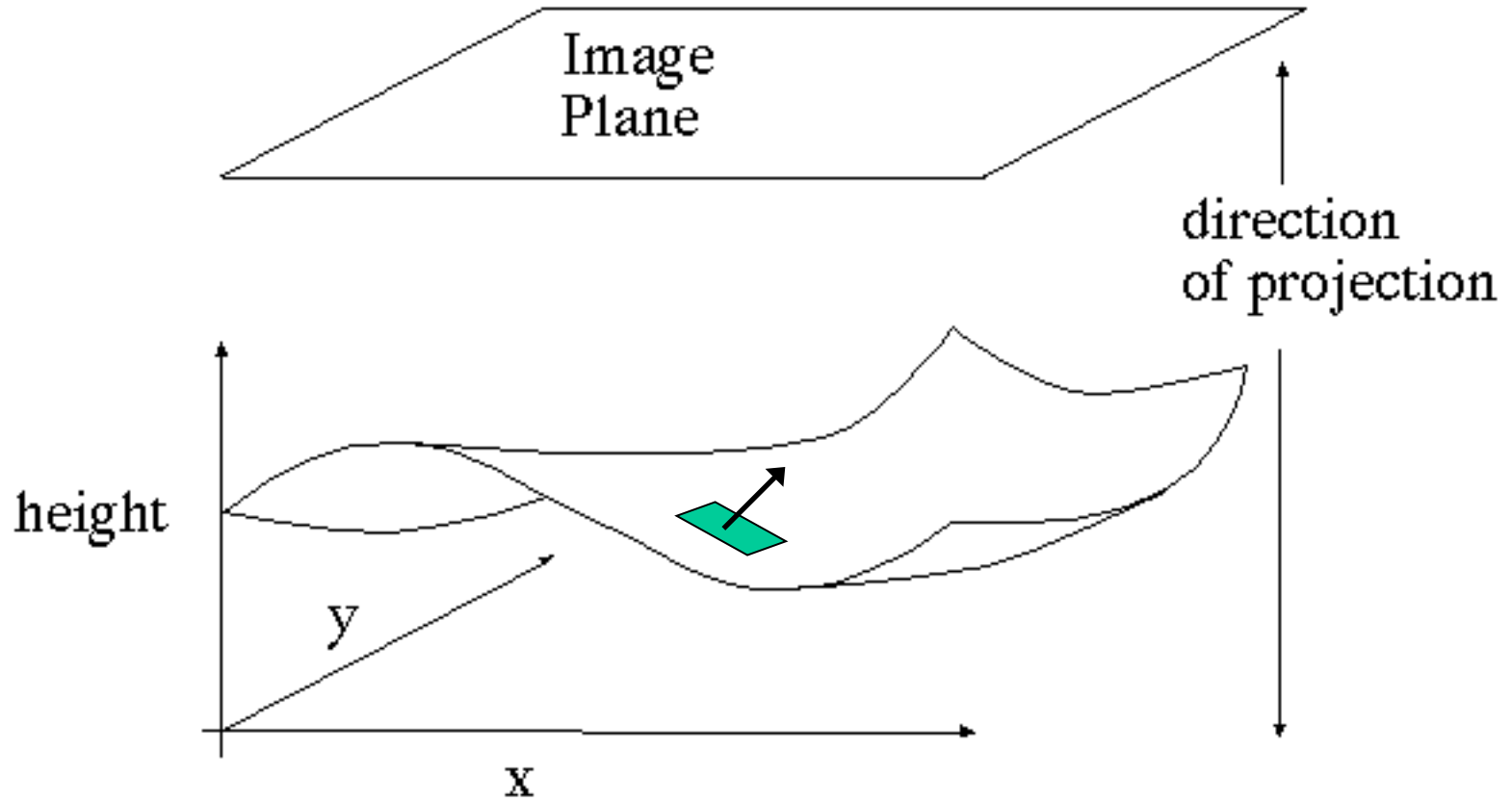


# Properties of object surfaces in range images



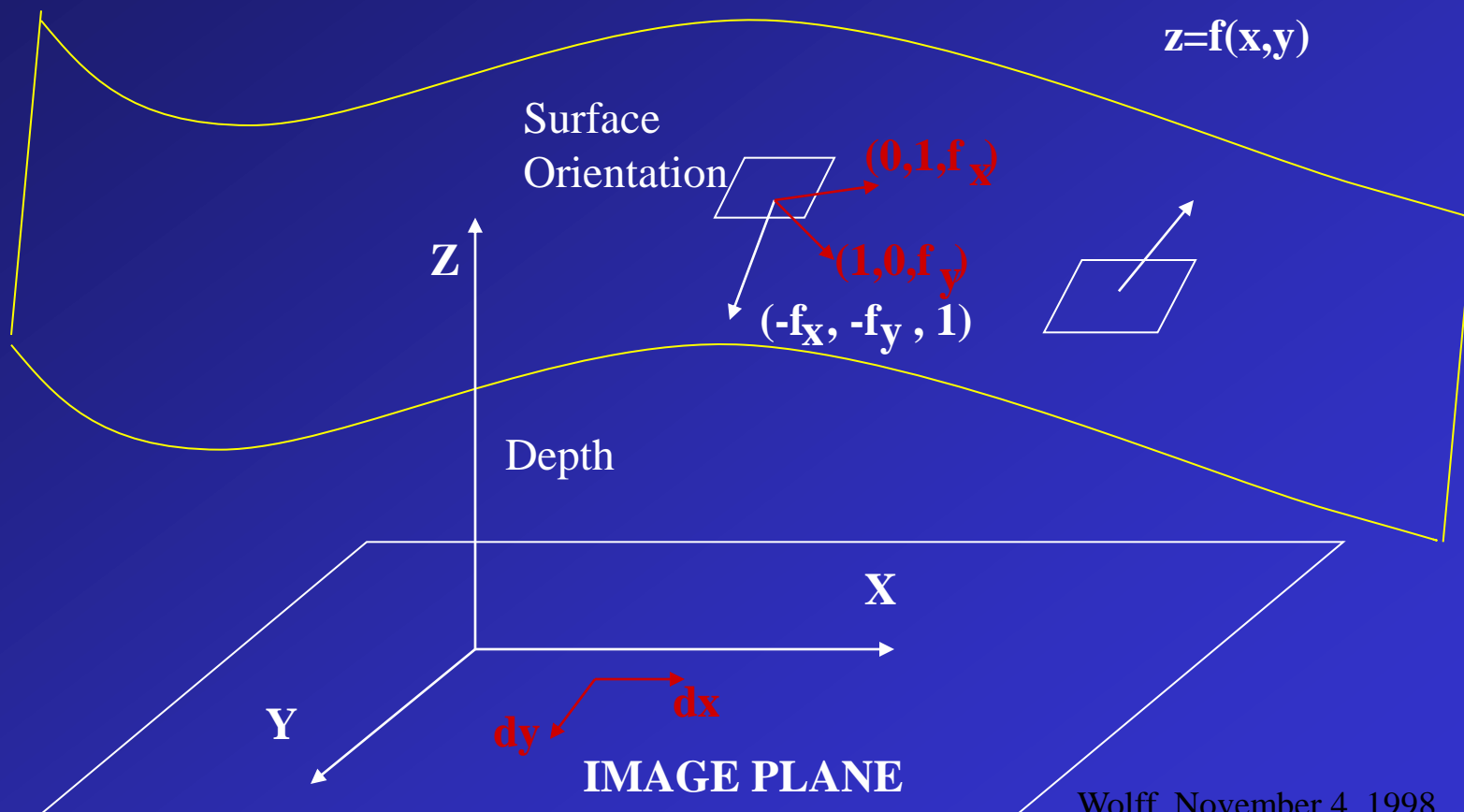
- Homogeneity of surface properties in:
  - Surface normals
  - Curvature
- Discontinuities between surfaces:
  - “roof edges”: locations with change of normals
  - “step edges”: discontinuous depth (e.g. hidden objects)

# Remember: Shape from Shading: "Monge" Patch



# Surface Orientation and Surface Normal

$$(f_x, f_y, -1) = (0, 1, f_x) \times (1, 0, f_y)$$



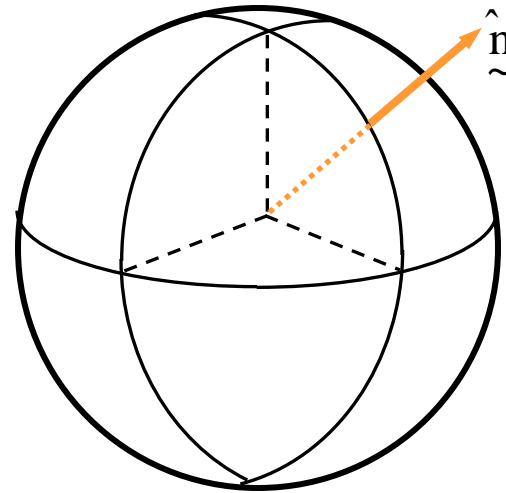
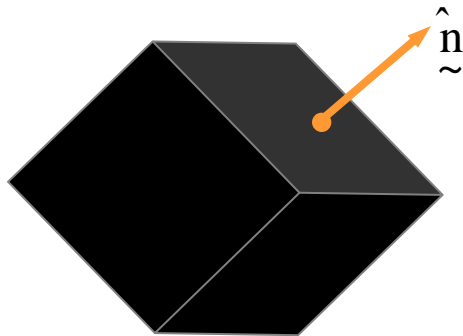
## Surface Orientation and Surface Normal

$$(-f_x, -f_y, 1) = (-p, -q, 1)$$

$p, q$  comprise a **gradient** or **gradient space** representation for local surface orientation.

# Object Representation: The Gaussian Image (EGI)

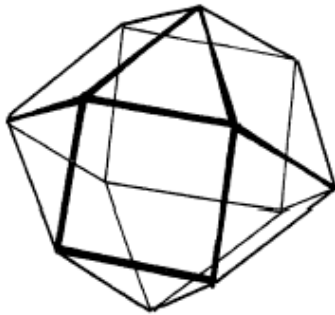
- Surface normal information for any object is mapped onto a unit (Gaussian) sphere by finding the point on the sphere with the same surface normal:





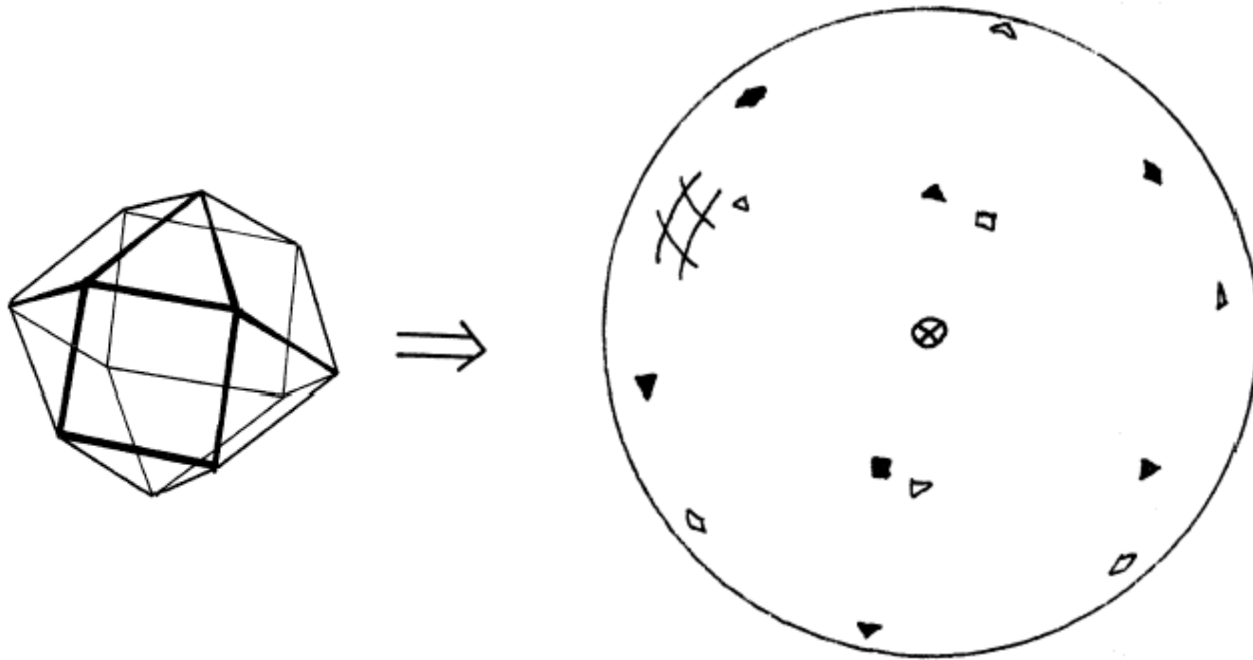


## Example (K. Horn)



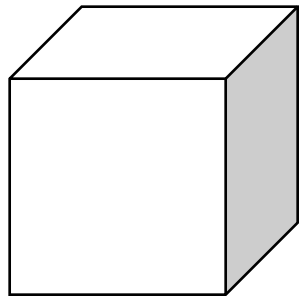


## Example (K. Horn)

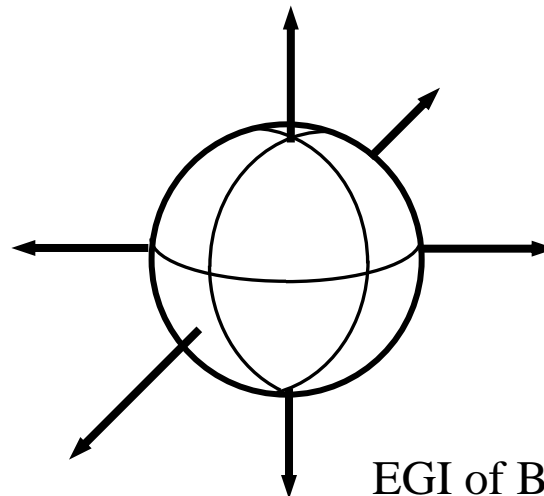


# The Extended Gaussian Image

- We can extend the Gaussian image by
  - placing a mass at each point on the sphere equal to the area of the surface having the given normal
  - masses are represented by vectors parallel to the normals, with length equal to the mass (**VOTING**)
- An example:



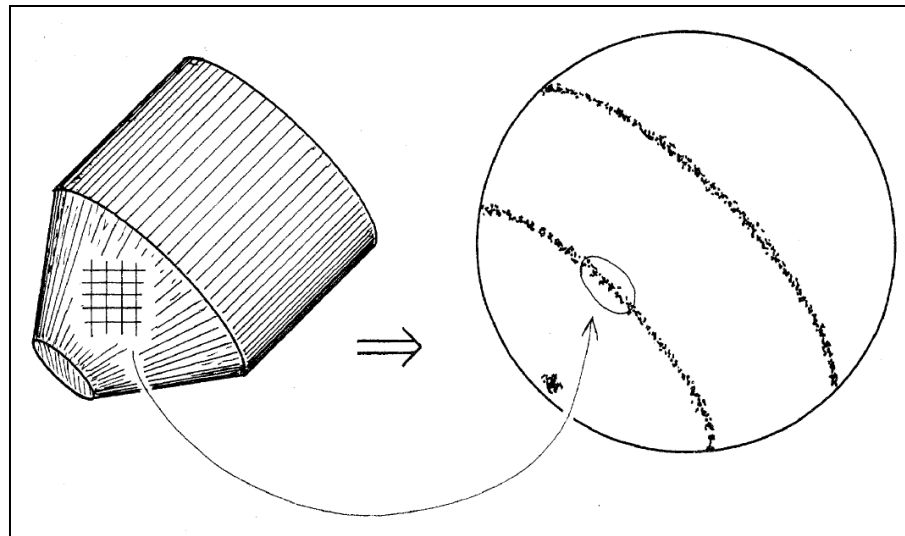
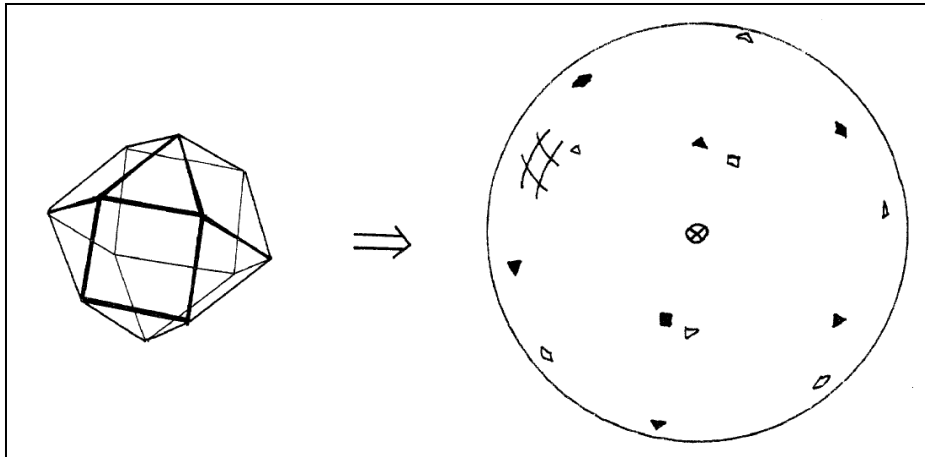
Block



EGI of Block



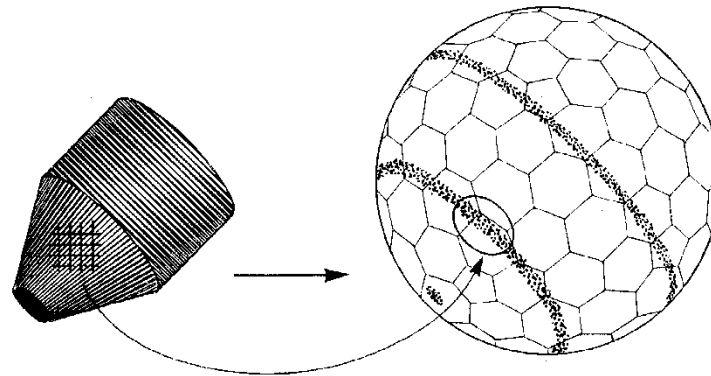
# K. Horn, MIT, 1983





# The Discrete Case EGI

- To represent the information of the Gaussian sphere in a computer, the sphere is divided into cells:



- For each image cell on the left, a surface orientation is found and **accumulated** in the corresponding cell of the sphere.

# Properties of the Gaussian Image



- This mapping is called the *Gaussian image* of the object when the surface normals for each point on the object are placed such that:
  - tails lie at the center of the Gaussian sphere
  - heads lie on the sphere at the matching normal point
- In areas of convex objects with positive curvature, no two points will have the same normal.
- Patches on the surface with zero curvature (lines or areas) correspond to a single point on the sphere.
- Rotations of the object correspond to rotations of the sphere.



# Using the EGI

- EGIs for different objects or object types may be computed and stored in a model database as a surface normal vector histogram.
- Given a depth image, surface normals may be extracted by plane fitting.
- By comparing EGI histogram of the extracted normals and those in the database, the identity and orientation of the object may be found.

# Properties of object surfaces in range images

- Homogeneity of surface properties in:
  - Surface normals
  - Curvature
- Discontinuities between surfaces:
  - “roof edges”: continuous depth but change of normals
  - “step edges”: discontinuous depth (e.g. hidden objects)





# Segmentation into planar patches

- F&P page 476/477
- Idea: Break object surface into sets of flat pieces
  - Clustering of surface normals via EGI
  - **Region growing**: Iterative merging of planar patches via graph/arc-costs



# Segmentation into planar patches

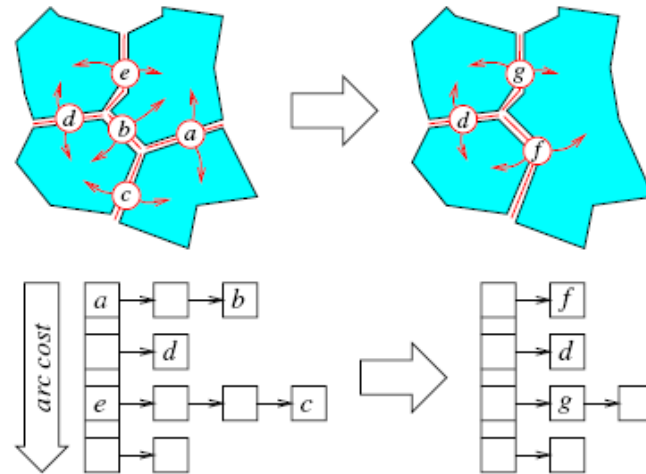


**Figure 24.11.** This diagram illustrates one iteration of the region growing process during which the two patches incident to the minimum-cost arc labelled *a* are merged. The heap shown in the bottom part of the figure is updated as well: the arcs *a*, *b*, *c* and *e* are deleted, and two new arcs *f* and *g* are created and inserted in the heap.

## Iterative merging of planar patches:

- Graph nodes: Patches with best fitting plane
- Graph arcs: costs corresponding to average error between combined set of points and plane that best fits these points
- Iteration: Find best arc, merge, next ...

# Segmentation into planar patches

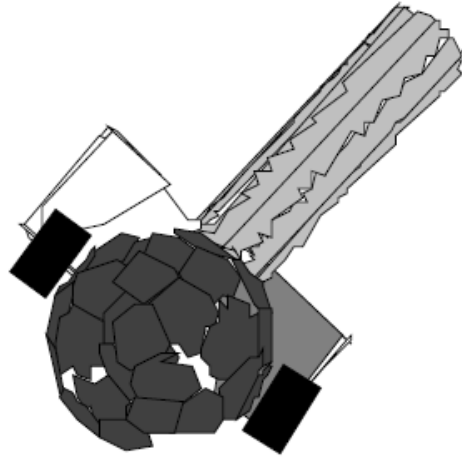


Figure 7: One of several grasping possibilities.

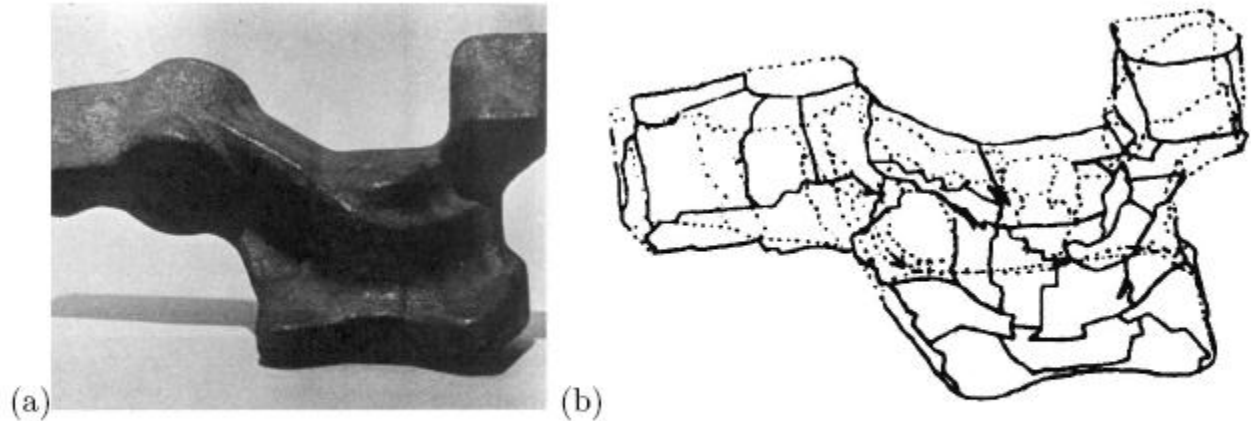
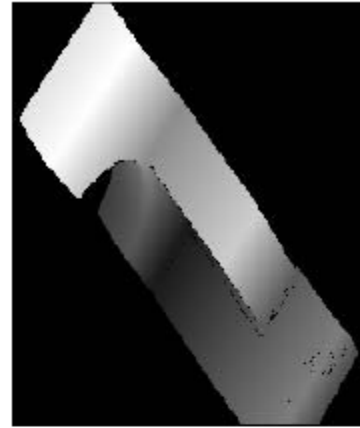
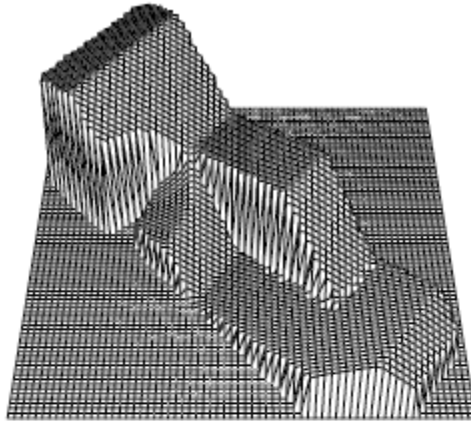
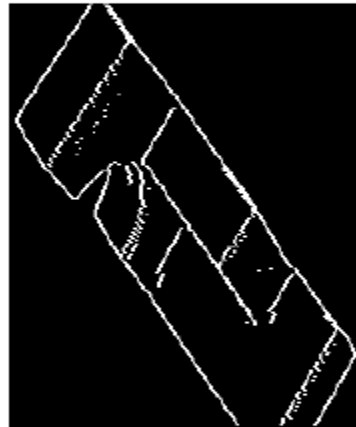


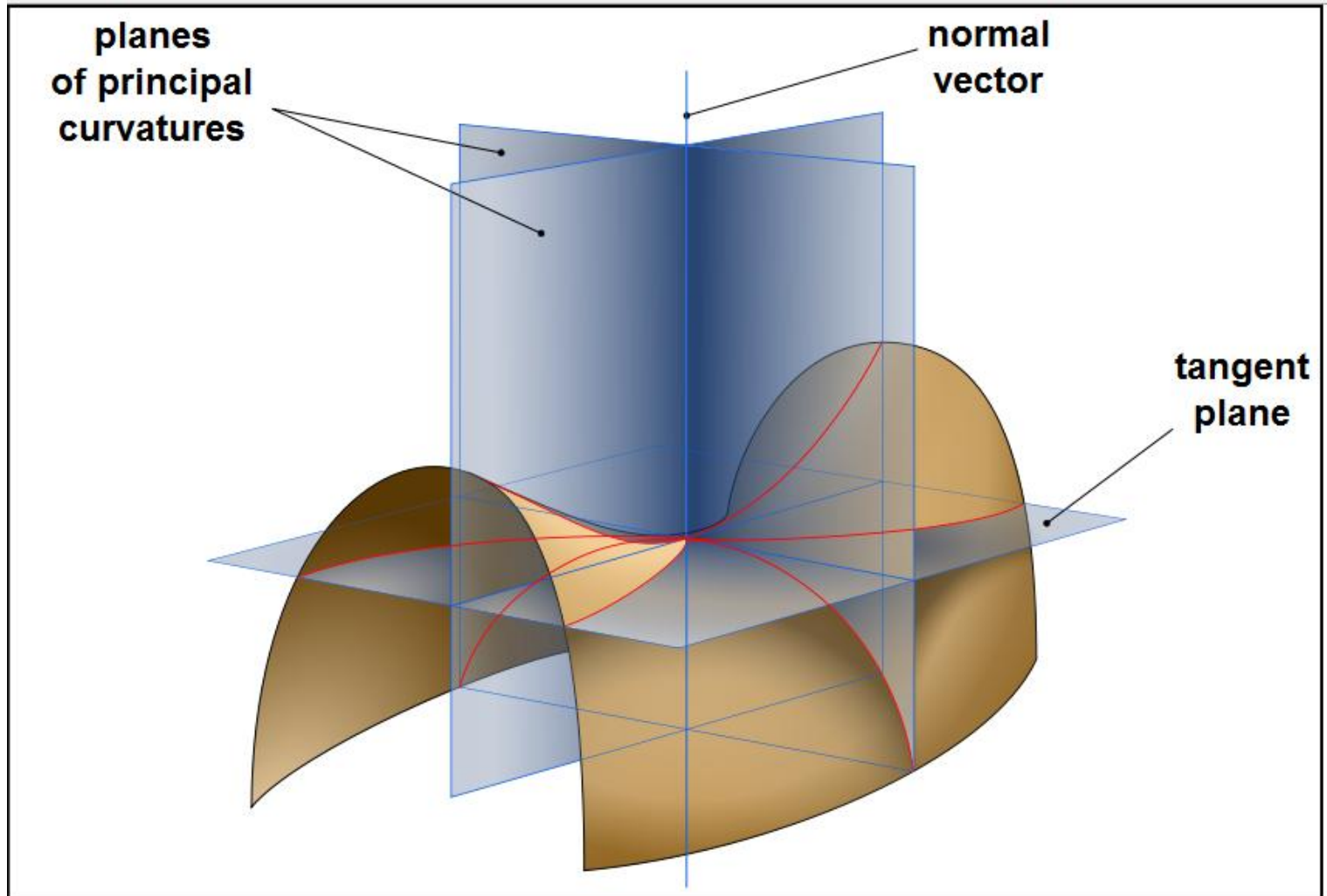
Figure 24.12. The Renault part: (a) photo of the part and (b) its model. Reprinted from [Faugeras and Hebert, 1986], Figures 1 and 6.



Segmentation  
into planar  
patches



# From flat pieces to curvature: Differential Geometry



# Elements of Analytical Differential Geometry (see F&P)

• Parametric surface:  $\mathbf{x} : U \times \mathbb{R}^2 \rightarrow \mathbb{R}^3$

• Unit surface normal:  $\mathbf{N} = \frac{1}{|\mathbf{x}_u \times \mathbf{x}_v|} (\mathbf{x}_u \times \mathbf{x}_v)$

• First fundamental form:

$$I(\mathbf{t}, \mathbf{t}) = Eu'^2 + 2Fu'v' + Gv'^2$$

$$\begin{cases} E = \mathbf{x}_u \cdot \mathbf{x}_u \\ F = \mathbf{x}_u \cdot \mathbf{x}_v \\ G = \mathbf{x}_v \cdot \mathbf{x}_v \end{cases}$$

• Second fundamental form:

$$II(\mathbf{t}, \mathbf{t}) = eu'^2 + 2fu'v' + gv'^2$$

$$\begin{cases} e = -\mathbf{N} \cdot \mathbf{x}_{uu} \\ f = -\mathbf{N} \cdot \mathbf{x}_{uv} \\ g = -\mathbf{N} \cdot \mathbf{x}_{vv} \end{cases}$$

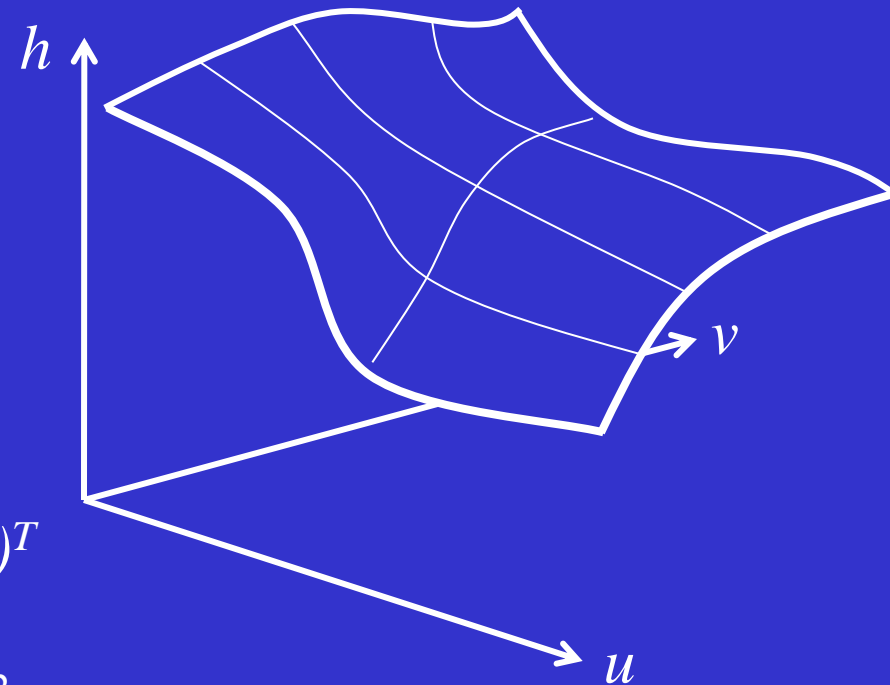
• Normal (direction  $\mathbf{t}$ ) and Gaussian curvatures:

$$\kappa_{\mathbf{t}} = \frac{II(\mathbf{t}, \mathbf{t})}{I(\mathbf{t}, \mathbf{t})}$$

$$K = \frac{eg - f^2}{EG - F^2}$$

## Example: Monge Patches

$$\mathbf{x}(u, v) = (u, v, h(u, v))$$



In this case

$$\bullet \mathbf{N} = \frac{1}{(1+h_u^2+h_v^2)^{1/2}} (-h_u, -h_v, 1)^T$$

$$\bullet E = 1+h_u^2; \quad F = h_u h_v; \quad G = 1+h_v^2$$

$$\bullet e = \frac{-h_{uu}}{(1+h_u^2+h_v^2)^{1/2}}; \quad f = \frac{-h_{uv}}{(1+h_u^2+h_v^2)^{1/2}}; \quad g = \frac{-h_{vv}}{(1+h_u^2+h_v^2)^{1/2}}$$

And the Gaussian curvature is:

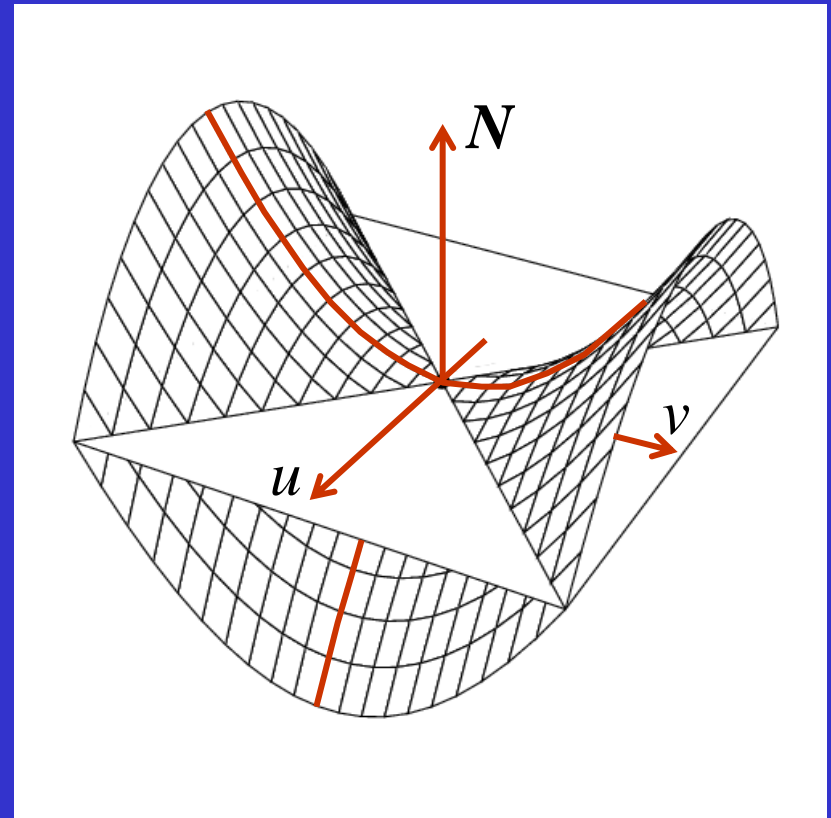
$$K = \frac{h_{uu}h_{vv} - h_{uv}^2}{(1+h_u^2+h_v^2)^2} .$$

## Example: Local Surface Parameterization

- $u, v$  axes = principal directions
- $h$  axis = surface normal

In this case:

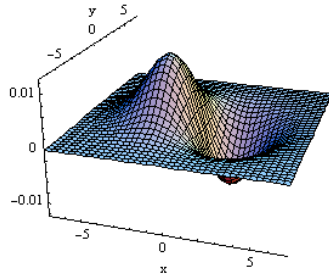
- $h(0,0)=h_u(0,0)=h_v(0,0)=0$
- $N=(0,0,1)^T$
- $h_{uv}(0,0)=0, \kappa_1 = -h_{uu}(0,0), \kappa_2 = -h_{vv}(0,0)$



Taylor expansion of order 2  $\longrightarrow h(u,v) = -\frac{1}{2} (\kappa_1 u^2 + \kappa_2 v^2)$



# Calculation of Partial Derivatives

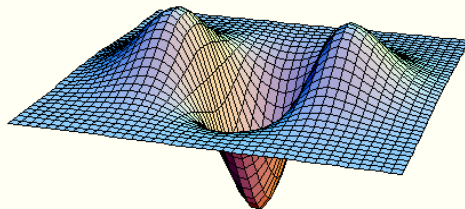


by convolving the smoothed image with the masks:

$$\frac{\partial}{\partial x} = \frac{1}{6} \begin{bmatrix} -1 & 0 & 1 \\ -1 & 0 & 1 \\ -1 & 0 & 1 \end{bmatrix} \quad \text{and} \quad \frac{\partial}{\partial y} = \frac{1}{6} \begin{bmatrix} 1 & 1 & 1 \\ 0 & 0 & 0 \\ -1 & -1 & -1 \end{bmatrix},$$

and the Hessian is computed by convolving the smoothed image with the masks

$$\frac{\partial^2}{\partial x^2} = \frac{1}{3} \begin{bmatrix} 1 & -2 & 1 \\ 1 & -2 & 1 \\ 1 & -2 & 1 \end{bmatrix}, \quad \frac{\partial^2}{\partial x \partial y} = \frac{1}{4} \begin{bmatrix} -1 & 0 & 1 \\ 0 & 0 & 0 \\ 1 & 0 & -1 \end{bmatrix} \quad \text{and} \quad \frac{\partial^2}{\partial y^2} = \frac{1}{3} \begin{bmatrix} 1 & 1 & 1 \\ -2 & -2 & -2 \\ 1 & 1 & 1 \end{bmatrix}.$$





# Principal Directions

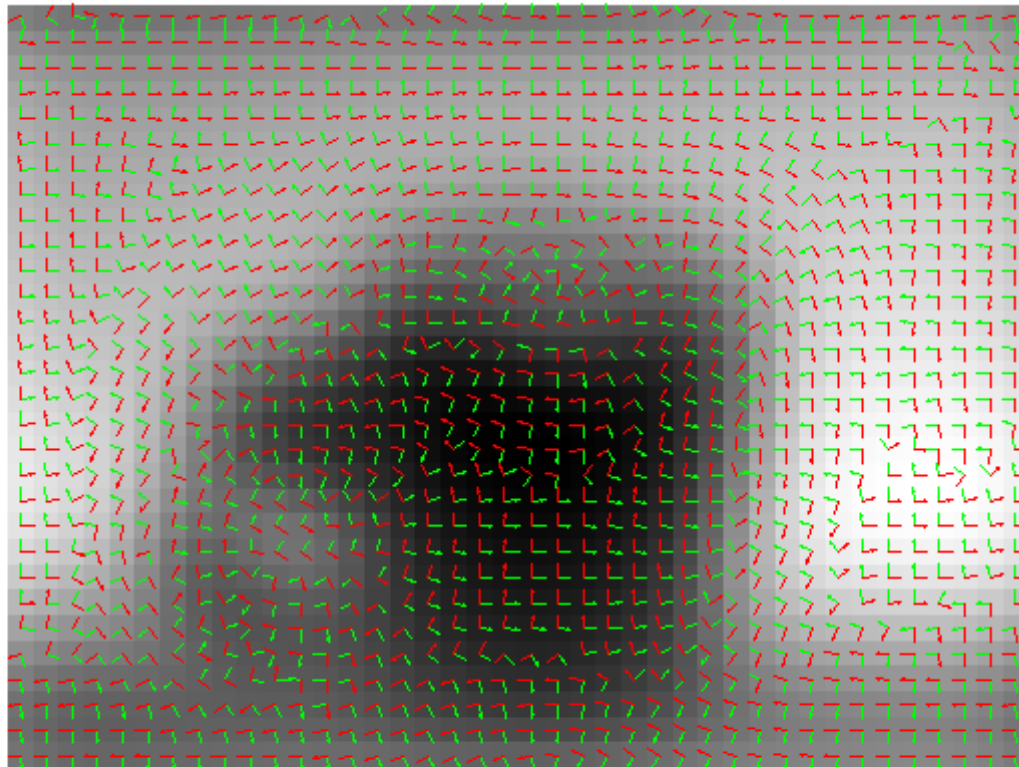
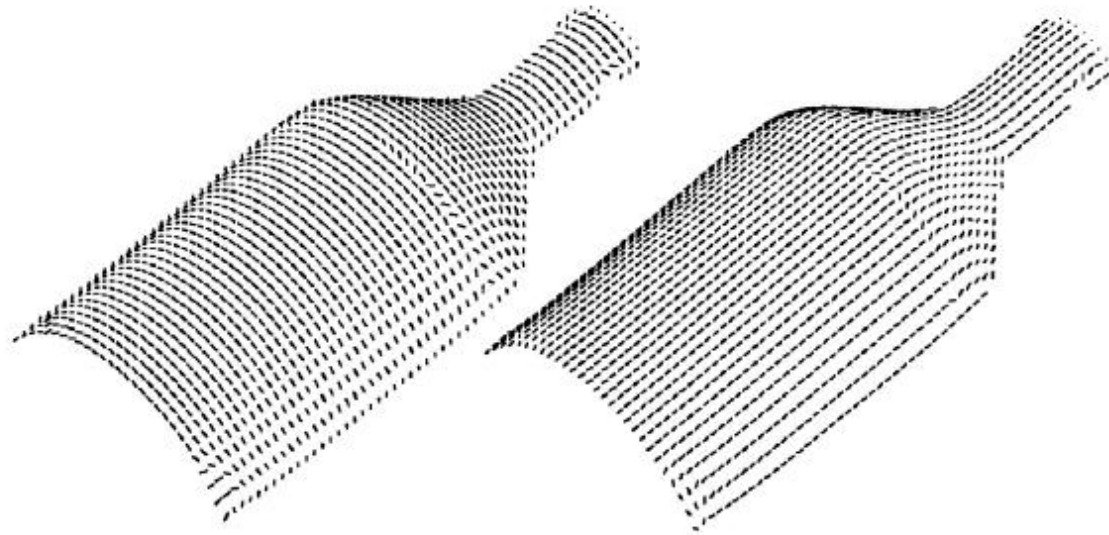


Figure 6.1 Frames of the normalized principal curvature directions at a scale of 1 pixel. Image resolution  $32^2$  pixels. Green: maximal principal curvature direction; red: minimal principal curvature direction.

# Calculation of principal curvatures

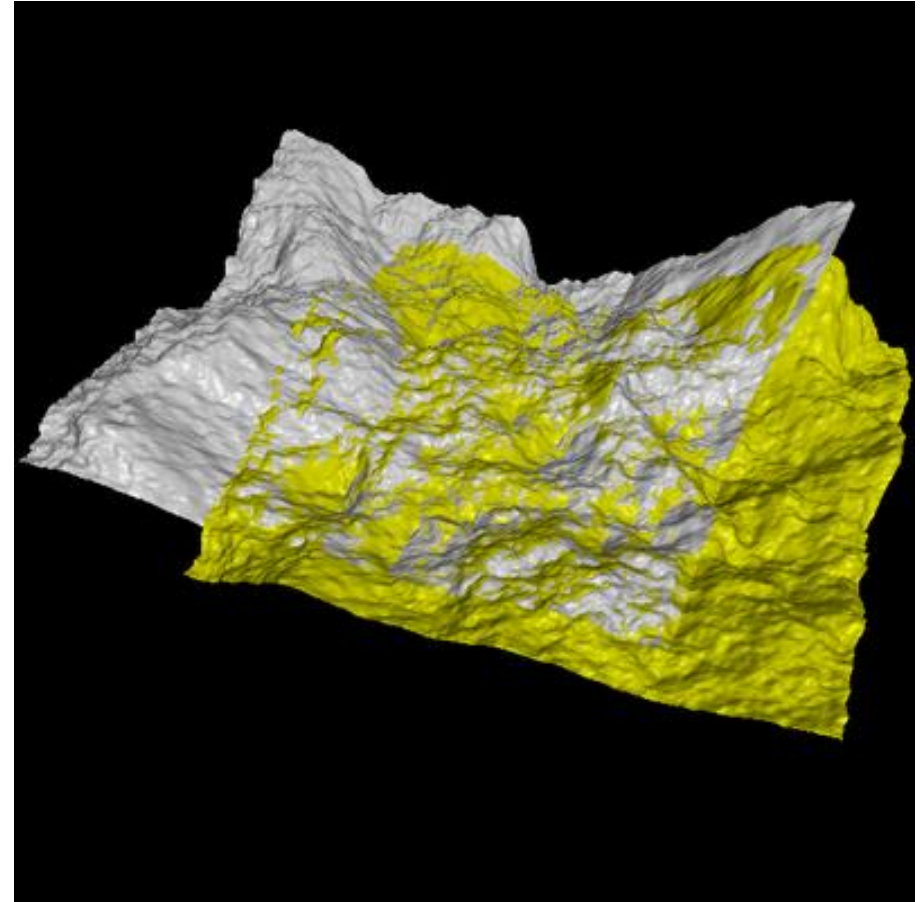


**Figure 24.8.** The two principal direction fields for the oil bottle. Reprinted from [Brady *et al.*, 1985], Figure 18.

Note that the principal curvatures are homogeneous across the large lower part of the bottle → **can serve as homogeneous features for clustering**

# The Problem

Align two  
partially-  
overlapping  
meshes  
given initial  
guess  
for relative  
transform



# Range Image Registration ctd.

- Concept:
  - Determine rigid transformation between pairs of range surfaces
  - Minimize average distance between point sets
  - **ICP**: **I**terative **C**losest **P**oint algorithm (Besl & McKay 1992)

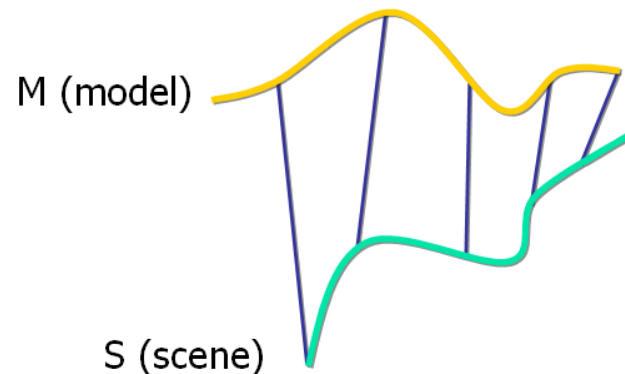


# Corresponding Point Set Alignment

- Let  $M$  be a model point set.
- Let  $S$  be a scene point set.

We assume :

1.  $N_M = N_S$ .
2. Each point  $S_i$  correspond to  $M_i$  .





# Corresponding Point Set Alignment

The MSE objective function :

$$f(R, T) = \frac{1}{N_s} \sum_{i=1}^{N_s} \|m_i - Rot(s_i) - Trans(s_i)\|^2$$

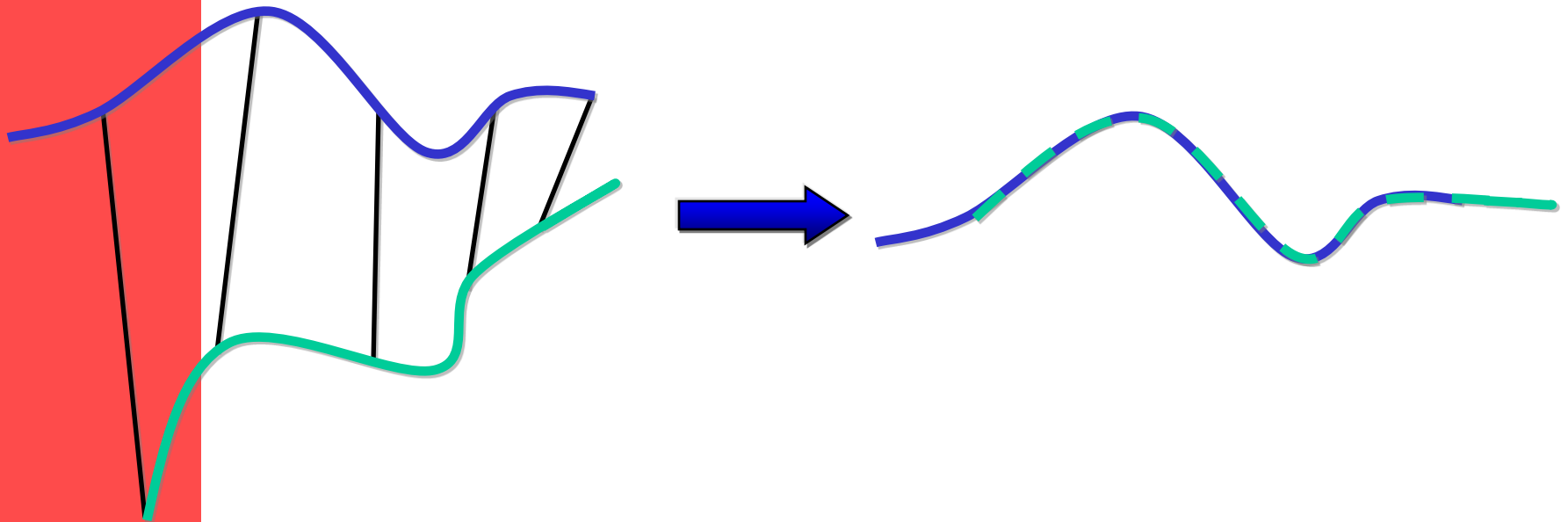
The alignment is :

$$(rot, trans, d_{mse}) = \Phi(M, S)$$



# Aligning 3D Data

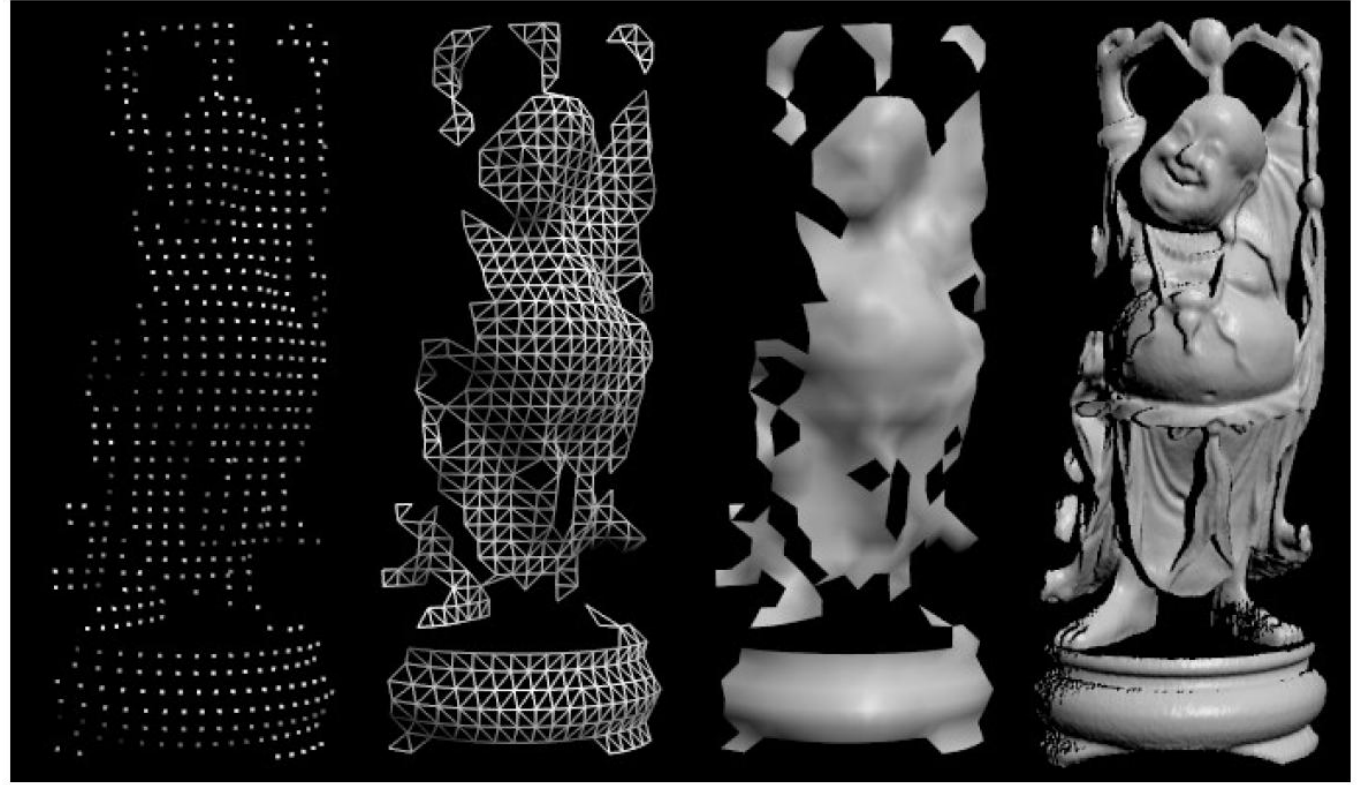
- If correct correspondences are known, can find correct relative rotation/translation





# Example: 3D Data Integration

- Range image registration

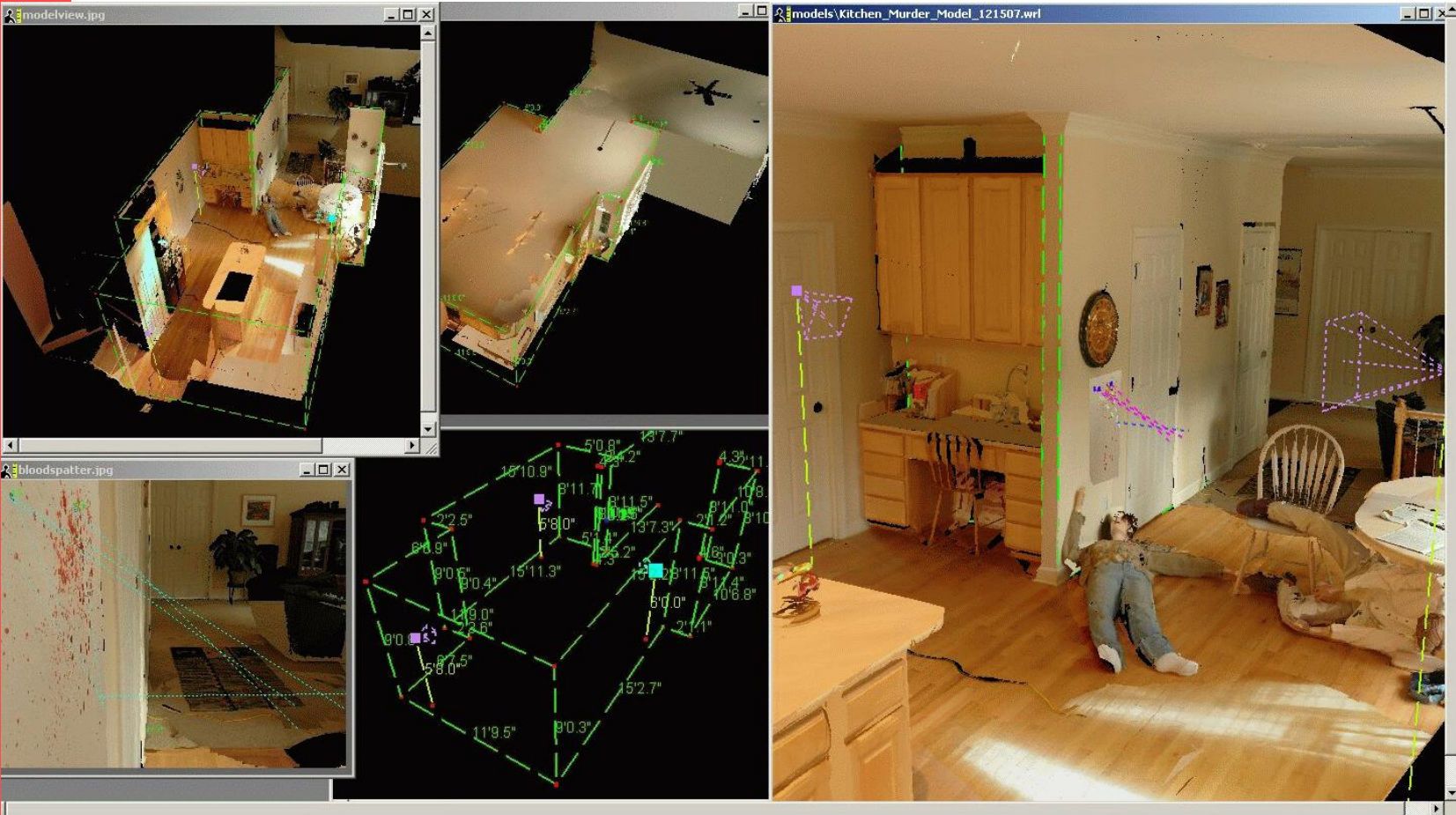


# Example: 3D Data Integration



**Figure 24.17.** 3D Fax of a statuette of a Buddha. From left to right: photograph of the statuette; range image; integrated 3D model; model after hole filling; physical model obtained via stereolithography. Reprinted from [Curless and Levoy, 1996], Figure 10.

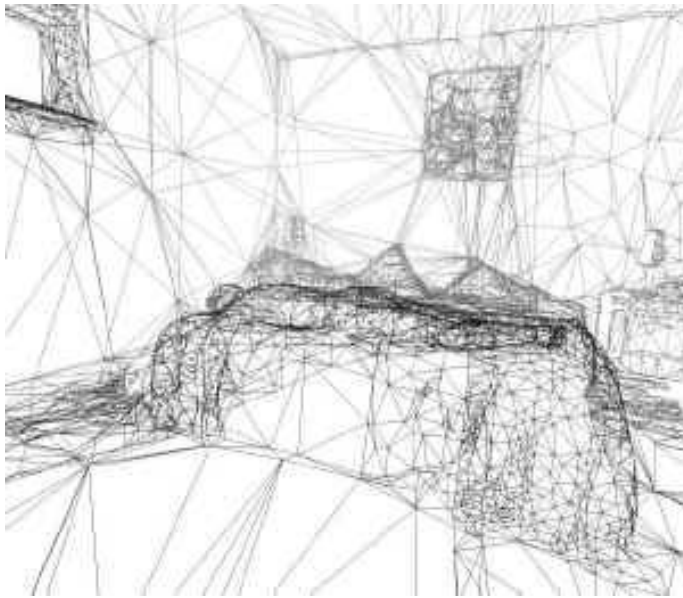
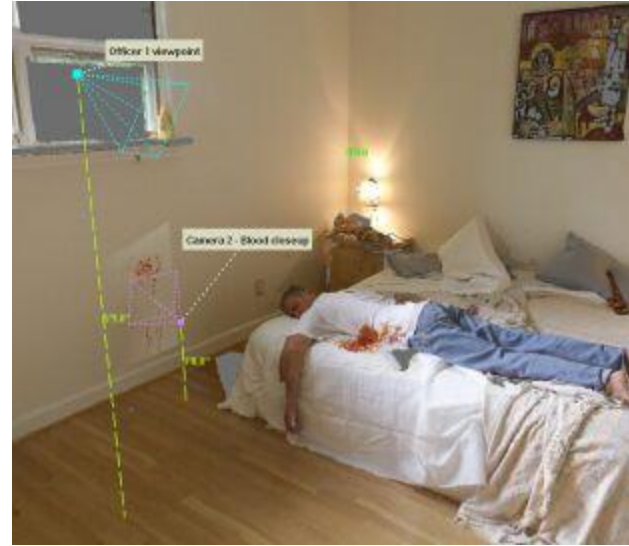
# Applications: Crime Scene, Forensic Analysis



<http://www.deltasphere.com/>



# Applications: Crime Scene, Forensic Analysis



<http://www.deltasphere.com/>

# Applications



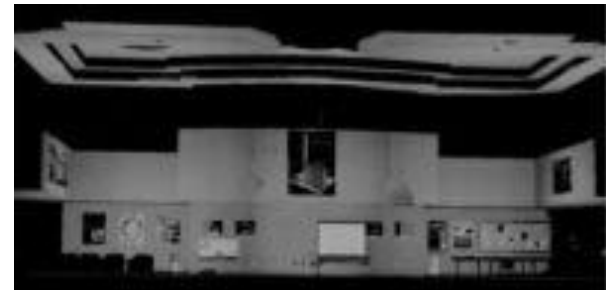
Museums, Cultural Exhibits



Archeology



Military Simulation and Training



Architecture and Construction

# Range Finders: Some References

- P.J. Besl. Active, optical range imaging sensors. *Machine Vision and Applications*, 1:127-152, 1988.
- R.A. Jarvis Range sensing for computer vision. In A.K. Jain and P.J. Flynn, editors, *Three-Dimensional Object Recognition Systems*, pages 17-56. Elsevier Science Publishers, 1993.
- T.G. Stahs and F.M. Wahl, "Fast and Robust Range Data Acquisition in a Low-Cost Environment", in *SPIE #1395: Close- Range Photogrammetry Meets Mach. Vis.*, Zurich, 1990, 496-503.



# Conclusions

## **Wide range of application areas including:**

- Action recognition and tracking
- Object pose recognition for robotic control
- Obstacle detection for automotive control
- Human-computer interaction
- Video surveillance
- Scene segmentation and obstacle detection
- Computer assisted surgical intervention
- Industrial applications of TOF cameras
- Automotive applications of TOF cameras
- Virtual reality applications
- Integration of range and intensity imaging sensor outputs





# References

- Horn, B.K.P. 1984. Extended Gaussian images. *In Proceedings of the IEEE 72*, 12 (Dec.), pp. 1656-1678.
- Horn, B.K.P. 1986. *Robot Vision*. MIT Press, Cambridge, MA, pp. 365-399.
- Kamvysselis, M. 1997. *2D Polygon Morphing using the Extended Gaussian Image.*  
<http://web.mit.edu/manoli/ecimorph/www/ecimorph.html>
- Kang, S.B. and K. Ikeuchi. 1990. *3-D Object Pose Determination Using Complex EGI*. tech. report CMU-RI-TR-90-18, Robotics Institute, Carnegie Mellon University.